MNRAS **000**, 1–13 (2015) Preprint 13 April 2021 Compiled using MNRAS LaTeX style file v3.0

# Supernova Siblings and their Parent Galaxies in the ZTF Bright Transient Survey

Melissa L. Graham[1★], Christoffer Fremling[2], Daniel A. Perley[3], Rahul Biswas[4], Christopher A. Phillips[1], Jesper Sollerman[4], Peter E. Nugent[5,6], Sarafina Nance[6,5], Suhail Dhawan[7], Jakob Nordin[8], Ariel Goobar[4], Adam Miller[9,10], James D. Neill[2], Xander J. Hall[2], and S. R. Kulkarni[2]
[1]*DiRAC Institute, Department of Astronomy, University of Washington, Box 351580, U.W., Seattle, WA 98195, USA*
[2]*Division of Physics, Mathematics, and Astronomy, California Institute of Technology, Pasadena, CA 91125, USA*
[3]*Astrophysics Research Institute, Liverpool John Moores University, IC2, Liverpool Science Park, 146 Brownlow Hill, Liverpool L3 5RF, UK*
[4]*The Oskar Klein Centre, Department of Astronomy, Stockholm University, SE-106 91 Stockholm , Sweden*
[5]*E.O. Lawrence Berkeley National Laboratory, 1 Cyclotron Rd., Berkeley, CA, 94720*
[6]*Department of Astronomy, University of California, Berkeley, CA 94720-3411, USA*
[7]*Institute of Astronomy and Kavli Institute for Cosmology, University of Cambridge, Madingley Road, Cambridge CB3 0HA, UK*
[8]*Institute of Physics, Humboldt-Universität zu Berlin, Newtonstr. 15, 12489 Berlin, Germany*
[9]*Center for Interdisciplinary Exploration and Research in Astrophysics and Department of Physics and Astronomy, Northwestern University, 1800 Sherman Ave, Evanston, IL 60201, USA*
[10]*The Adler Planetarium, Chicago, IL 60605, USA*

Accepted XXX. Received YYY; in original form ZZZ

## ABSTRACT

Supernova (SN) siblings – two or more SNe in the same parent galaxy – are useful tools for exploring progenitor stellar populations as well as properties of the host galaxies such as distance, star formation rate, dust extinction, and metallicity. Since the average SN rate for a Milky Way-type galaxy is just one per century, a large imaging survey is required to discover an appreciable sample of SN siblings. From the wide-field Zwicky Transient Facility (ZTF) Bright Transient Survey (BTS; which aims for spectroscopic completeness for all transients which peak brighter than $r$<18.5 mag) we present 10 SN siblings in 5 parent galaxies. For each of these families we analyze the SN's location within the host and its underlying stellar population, comparing with expectations that SNe from more massive progenitors are found nearer to their host core and in regions of more active star formation. We also present an analysis of the relative rates of core collapse and thermonuclear SN siblings, finding a significantly lower ratio than past SN sibling samples due to the unbiased nature of the ZTF.

**Key words:** transients: supernovae – surveys

## 1 INTRODUCTION

It has long been known that some galaxies are more efficient at producing supernovae than others. In describing their choice of fields to survey in order to generate a large sample of supernovae, Zwicky (1938) focus on galaxies in nearby clusters (i.e., where a single field of view can contain a large stellar mass), and on star-forming galaxies such as those similar to the Andromeda Galaxy (grand design spirals) and those with low-surface brightness, which offer the additional bonus of being easy to search by eye. Such a focus is effective, especially when survey étendue[1] is limited, however this strategy can miss entire populations of transient events (i.e., those which are hostless or in galaxies of low stellar mass), and does not work well for high-redshift cosmological applications.

The Zwicky Transient Facility (ZTF; Graham et al. 2019; Bellm et al. 2019; Masci et al. 2019) is a modern wide-field optical sky survey which does not need to target individual galaxies thanks to its 47 deg$^2$ field of view. The ZTF is a public-private partnership survey which uses the 48 inch telescope at Palomar Observatory to image the entire northern sky once every $\sim$ 3 days in the $g$ and $r$ filters to a depth of $r \sim 20.5$ mag. Discoveries made in the public data are released as alerts, and available via the public alert brokers such as AMPEL[2], ANTARES[3], ALeRCE[4], and Lasair[5]. Dedicated time on the Palomar Observatory 60 and 200 inch telescopes, the former with the SED Machine instrument (SEDM; Blagorodnova et al. 2018; Rigault et al. 2019), is used for follow-up and classification of ZTF discoveries. In particular, the ZTF Bright Transient Survey (BTS; Fremling et al. 2020; Perley et al. 2020a) applies a filter to the ZTF public survey alert stream to identify and spectroscopically classify, with very high completeness, transients with a peak apparent brightness of $r \leq 18.5$ mag. The BTS follow-up strategy is to target all likely SNe detected by ZTF that are brighter than 19 mag in the $g$ or $r$ filter, and then

---

★ E-mail: mlg3k@uw.edu

[1] The product of the camera's field of view and the telescope's aperture.

[2] `https://ampelproject.github.io/`

[3] `https://antares.noirlab.edu/`

[4] `https://alerce.online/object/ZTF20aavpwxl`

[5] `https://lasair.roe.ac.uk/`

raising the priority for targets brighter than 18.5 mag, with the goal of obtaining spectra for all objects brighter than 18.5 (unless prevented by, e.g., bad weather or technical issues). As described in Perley et al. (2020a), this strategy lead to a spectroscopic completeness rate of 93% (75%) for SNe brighter than 18.5 (19) mag.

In such large modern surveys it remains true that some galaxies appear to be more prolific producers of SNe, through a combination of galaxy properties and chance. SNe which occur in the same host galaxy are referred to as “siblings", and their common host the “parent" galaxy. These SN siblings are more than just a novelty – they provide unique scientific opportunities. Thöne et al. (2009) study three SN siblings all classified as Type Ib (1999eh, 2007uy, 2008D) in NGC 2770, a spiral galaxy similar to the Milky Way. They use spectra of the parent galaxy to show that the sites of the SNe Ib had subsolar metallicities (but that random chance could not be ruled out as the reason why all three were of the rare SN Ib subtype). Anderson & Soto (2013) compile and analyze a large sample of SN siblings and use the ratio of different types, such as core-collapse supernovae (CC SNe; explosions of $>8$ $M_\odot$ stars) and Type Ia supernovae (SNe Ia, the thermonuclear explosions of white dwarf stars) to constrain the average duration of star-formation episodes. We discuss their work in more detail in Section 4.

Supernovae are used as cosmological probes, and siblings in the same parent galaxy can be used to study the systematic contribution in their distance estimates. Gall et al. (2018) show that the fast-declining SN Ia siblings 2007on and 2011iv yield distance estimates to NGC 1404 that are, surprisingly, discrepant by up to 14%. Burns et al. (2020) find that the slow-declining SN Ia siblings 2013aa and 2017cbv are nearly identical in their light curves and spectra (although 13aa was not discovered early enough to detect a “blue bump" like 17cbv; Hosseinzadeh et al. 2017). They also show that host-galaxy distances from sibling SNe Ia are consistent to within 3% (*vs.* 6% among non-siblings). Scolnic et al. (2020) used 16 SN Ia siblings from the Dark Energy Survey to show that up to half of the intrinsic scatter in SN Ia peak brightness could be attributed to host galaxy properties – and thus potentially be corrected for in cosmological applications.

In this work we search the ZTF BTS sample for SN siblings and find five pairs, which are presented in Section 2. We provide individual analyses of these pairs and their host galaxies in Section 3, examining the SN locations within their hosts, the underlying stellar populations, and in some cases comparing the distance estimates that we have derived from the SN light curves. In Section 4 we provide a relative rates analysis for different sibling types, and discuss how the results from an unbiased survey like ZTF compare with past studies. We summarize our conclusions in Section 5.

## 2 SN SIBLING IDENTIFICATION AND OBSERVATIONS

For this work we begin with all ZTF transients that passed the BTS filter as of Sep 13 2020, which includes all events – classified and unclassified – that were, at any point in their light curve, brighter than $r = 19$th magnitude. This sample was generated using the BTS Explorer webpage (Perley et al. 2020a)[6], with the quality and purity cuts applied. The quality filter removes candidates which occurred at times or in regions of poor observability, and the purity filter removes objects that are highly likely to be false positives (non-supernova transients). We allow our sample to extend one month earlier and one month later than the start and end dates imposed by Perley et al. (2020a). Thus we start with a total of 2640 objects, 148 more than the total of all transients and unclassified objects quoted in Table 1 of Perley et al. (2020a). Most of the additional candidates are SNe Ia and unclassified transients, the two most populous categories. In this sample we identified 46 transients that were within 250″ of each other, and another 4 transients with a redshift limit of $z < 0.0050$ that were within 250–600″ of each other. All 4 events in the latter group were M31 novae, as were 4 in the previous group, for a total of 8 M31 novae, and 42 potential siblings.

We visually reviewed images of these 42 potentially associated transients (21 pairs) to identify true siblings, and the results of this visual review are presented in Table 1. In the top section of Table 1 we list the 20 SNe (10 pairs) that we confirm are siblings because they obviously appear in the same parent galaxy. In the middle section, we list 6 SNe (3 pairs) that do not appear in the same host galaxy, and are not siblings, but which might be “cousins" (i.e., their hosts belong to the same group or cluster of galaxies, or their progenitor system might be an intragroup or intracluster star). In the bottom section of Table 1 we list 16 transients (8 pairs) that are within 250″ of each other but do not appear to be physically associated (i.e., are chance alignments). The 8 novae in M31 which met the BTS criteria are not listed in Table 1[7].

For our 20 identified SN siblings which passed the BTS filter (10 pairs), we list their SN type, redshift, and brightest observed magnitude in Table 2. Of these 20 objects, nine have peak observed brightnesses fainter than 18.5 mag (denoted by asterisks in columns four and eight). The 5 sibling pairs in the BTS sample of SNe with a peak brightness of $<18.5$ mag – for which Perley et al. (2020a) demonstrates a spectroscopic completeness of 93% – are all listed above the horizontal line in Table 2, and we focus the analysis in this paper on them. For these 5 SN sibling pairs, Figure 1 marks the location of each SN in the parent galaxy ($g$ band images from the PanSTARRS image cutout server; Chambers et al. 2016; Magnier et al. 2020). Figure 2 shows the ZTF public light curve data, and Figure 3 shows the BTS follow-up spectroscopy with the P60+SEDM which provided the spectroscopic classifications. Each sibling pair is discussed in more detail in Section 3

In the BTS sample of SNe with peak brightness $<18.5$ ($<19$) mag, we found that only 9 (16) out of 10 (20) SN siblings were spectroscopically classified. These fractions are not a cause for alarm – they match the overall spectral completeness for the full BTS sample of SNe, 75% (93%) for SNe with peak brightness $<19$ ($<18.5$) mag (Perley et al. 2020a). The classification of SN 2019abo as *SNI?* is discussed in Section 3.5, and the classifications for SNe with peak brightnesses $<19$ mag are discussed in Sections 2.1 to 2.3.

### 2.1 Classification for SN 2019svq (ZTF19acgaxei)

SN 2019svq does not have much of a light curve, as it was detected in only three epochs, all of them $r$ band. The rise-time was at least 8 days. Multiple epochs of spectroscopy were obtained with both the P60+SEDM and the P200 telescopes, but all spectra appear to be host dominated. The spectral type of SN 2019svq remains unclear.

---

[6] `https://sites.astro.caltech.edu/ztf/bts/explorer.php`

[7] They are: ZTF19abirmkt, ZTF19abtrjqg, ZTF19acbzgog, ZTF19acgfhfd, ZTF19acnfsij, ZTF19acqprad, ZTF19adakuos, and ZTF20abqhsxb.

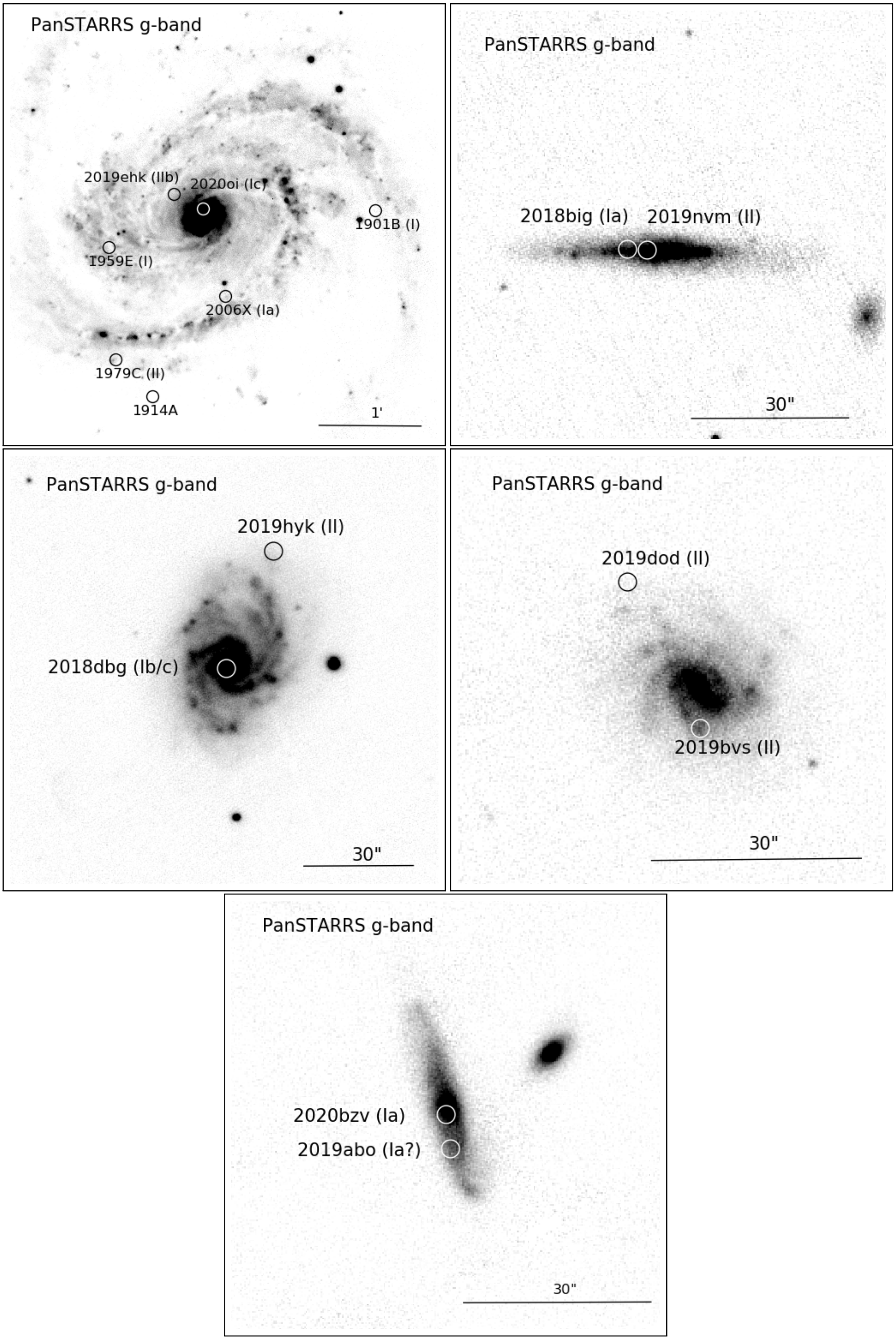

**Figure 1.** Image stamps showing the locations of the five SN sibling pairs with peak observed brightnesses $<18.5$ mag. All are north-up, east-left $g$ band images from the PanSTARRS image cutout server, with a linear scaling set to emphasize the host features. Circles mark the locations of SN siblings, as labeled. SN classifications are included in the labels where possible.

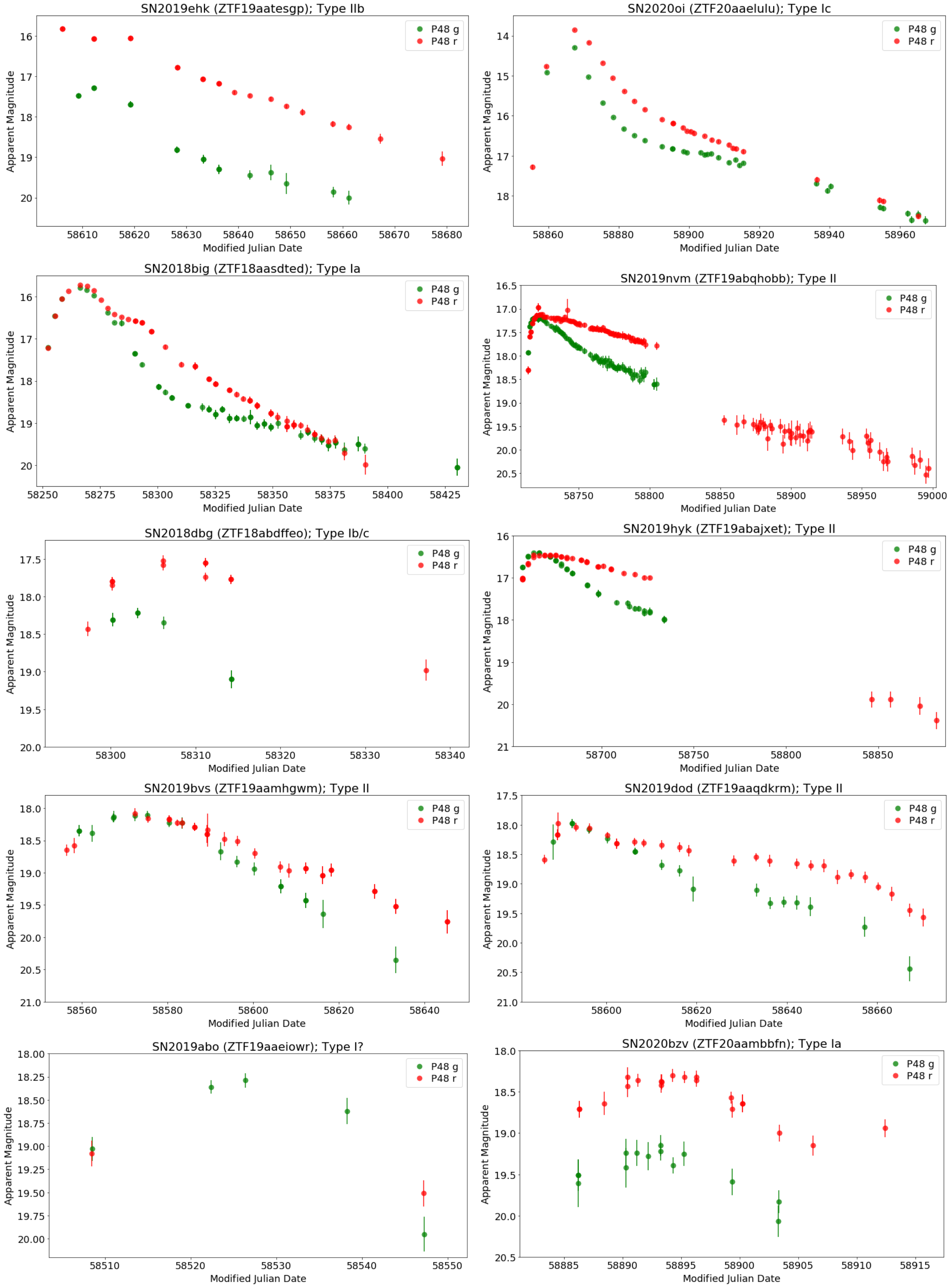

**Figure 2.** Light curves of SN siblings (one pair per row) with peak observed magnitude ≤ 18.5 mag in either the *g* or *r* filter. Plots show ZTF P48 photometry in *g* and *r* bands (green and red points respectively) from the public data set. Photometry for SN 2019ehk was published by De et al. (2020a), and for SN 2020oi by Horesh et al. (2020).

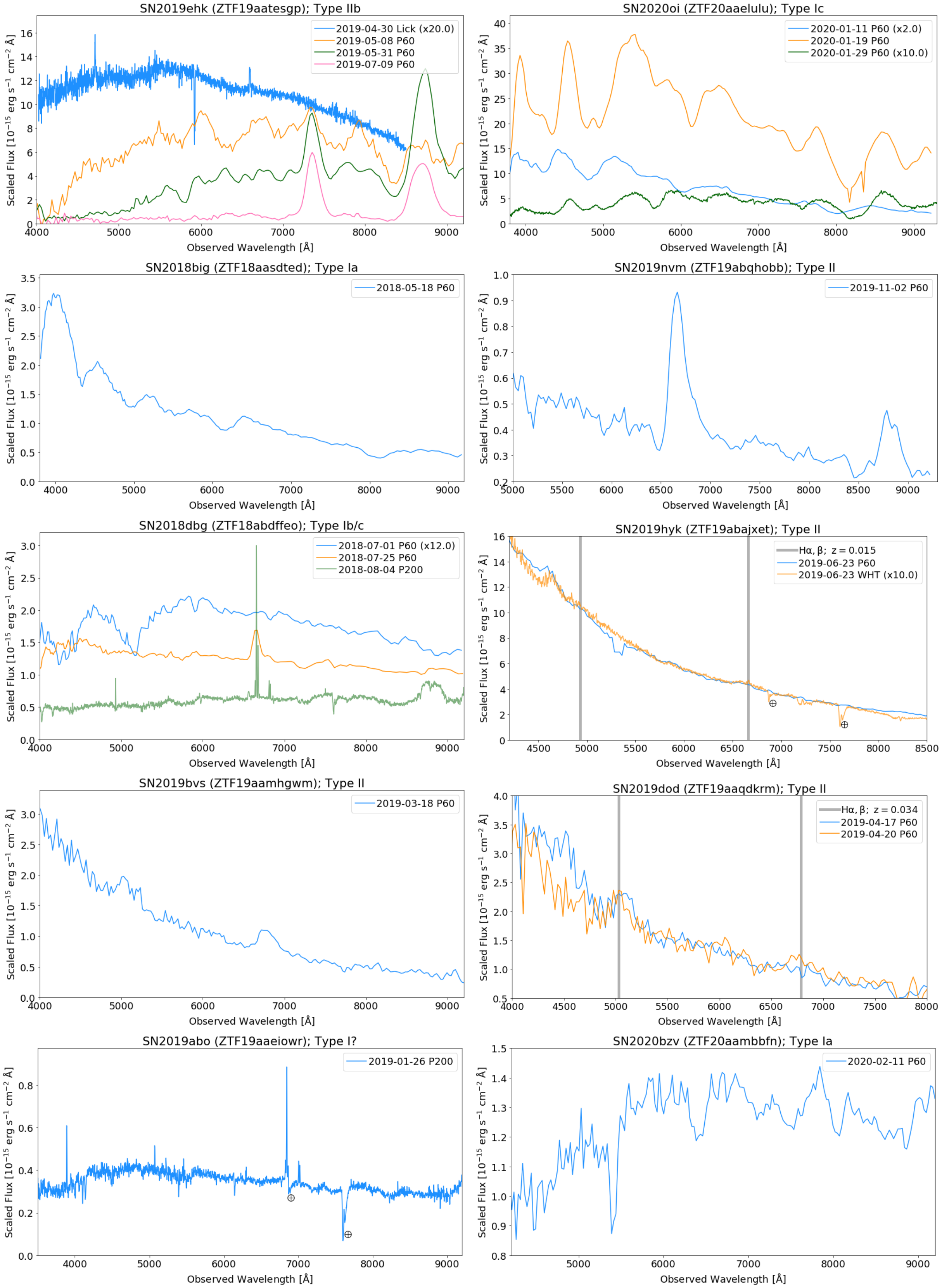

**Figure 3.** Selected epochs of P60+SEDM (or P200) spectroscopy that are relevant to the classification of SN siblings with peak observed magnitude ≤ 18.5 mag in either the $g$ or $r$ filter. For SN 2019ehk we also include the classification spectrum from Lick Observatory (Dimitriadis et al. 2019). For SN 2018dbg, the 2018-08-04 spectrum was published in De et al. (2020a). For SN 2019hyk, we also include the classification spectrum from the William Herschel Telescope (WHT; Fraser et al. 2019).

**Table 1.** The results of a visual review of sibling candidates, sorted by on-sky separation distance and listed in three categories: (top) SNe that we identified as siblings, (middle) SNe whose hosts might be physically associated, and (bottom) chance alignments.

| Separation (″) | ZTF Names | | Comments regarding visual review. |
|---|---|---|---|
| *Identified siblings:* | | | |
| 3.7 | ZTF18aasdted | ZTF19abqhobb | same parent galaxy |
| 5.6 | ZTF19aaeiowr | ZTF20aambbfn | same parent galaxy |
| 5.6 | ZTF19aaksrgj | ZTF20aavpwxl | same parent galaxy |
| 5.7 | ZTF19abgrchq | ZTF19acgaxei | same parent galaxy |
| 8.6 | ZTF19accobqx | ZTF19acnwelq | same parent galaxy |
| 19.8 | ZTF19aatesgp | ZTF20aaelulu | same parent galaxy |
| 23.8 | ZTF19aamhgwm | ZTF19aaqdkrm | same parent galaxy |
| 24.3 | ZTF18aboabxv | ZTF18adachwf | same parent galaxy |
| 35.7 | ZTF18abdffeo | ZTF19abajxet | same parent galaxy |
| 42.4 | ZTF19aavitlq | ZTF19abpyqog | same parent galaxy |
| *Not siblings, but hosts might be associated:* | | | |
| 50.1 | ZTF19aaekvwv | ZTF19acnqsui | *qsui* might be hostless in a cluster with *kvwv* host |
| 106.1 | ZTF19acykqyr | ZTF20abiserv | *kqyr* is distant from group hosting *serv*, but at $z$; tidal stream? |
| 133.8 | ZTF18abdbysy | ZTF20aaurjzv | *rjzv* host might be a satellite galaxy of *bysy* host |
| *Not siblings, and not likely to be associated:* | | | |
| 46.8 | ZTF18abqkfvr | ZTF19aanuipj | *kfvr* appears hostless, might be high-$z$ (unclassified) |
| 70.4 | ZTF19aauxmqj | ZTF19abeloei | different hosts; hosts appear to be unassociated (i.e. different $z$) |
| 142.1 | ZTF19aavhypb | ZTF18aaizerg | different hosts; hosts appear to be unassociated (i.e. no obvious cluster) |
| 149.6 | ZTF19aafmymc | ZTF20aazstdx | different hosts; hosts appear to be unassociated (i.e. different $z$) |
| 202.8 | ZTF18acxgoki | ZTF19abqgtqo | different hosts; hosts appear to be unassociated (i.e. no obvious cluster) |
| 224.7 | ZTF19aarflsx | ZTF20aahggbm | different hosts; hosts appear to be unassociated (i.e. no obvious cluster) |
| 237.0 | ZTF19aaeoqst | ZTF19aafndoy | different hosts; might be in the same cluster |
| 246.4 | ZTF19acjndrx | ZTF19acjndsa | both are apparently hostless (might be high-$z$) |

**Table 2.** Properties of the 20 SNe we identified as siblings. The horizontal line separates the SN siblings for which the brightest observed apparent magnitudes of both events were brighter/fainter than 18.5 mag.

| ZTF Name | IAU Name | Spectral Type | Redshift (Host or SN) | Brightest Magnitude* | ZTF Name | IAU Name | Spectral Type | Redshift (Host or SN) | Brightest Magnitude* |
|---|---|---|---|---|---|---|---|---|---|
| 19aatesgp | 2019ehk | SNIIb | 0.0055 | $r = 15.82$ | 20aaelulu | 2020oi | SNIc | 0.0052 | $r = 13.86$ |
| 18aasdted | 2018big | SNIa | 0.0181 | $r = 15.72$ | 19abqhobb | 2019nvm | SNII | 0.0181 | $r = 17.12$ |
| 18abdffeo | 2018dbg | SNIb/c | 0.0148 | $r = 17.52$ | 19abajxet | 2019hyk | SNII | 0.0147 | $g = 16.41$ |
| 19aamhgwm | 2019bvs | SNII | 0.0342 | $r = 18.08$ | 19aaqdkrm | 2019dod | SNII | 0.0342 | $g = 17.98$ |
| 19aaeiowr | 2019abo | *SNI?* | 0.0432 | $g = 18.29$ | 20aambbfn | 2020bzv | SNIa | 0.0439 | $r = 18.30$ |
| 19abgrchq | 2019lsk | SNIIb | 0.0300 | $r = 18.16$ | 19acgaxei | 2019svq | - | 0.0297 | $r = 18.97$* |
| 19accobqx | 2019sik | SNIa | 0.1000 | $g = 18.52$* | 19acnwelq | 2019uej | *SNIa?* | *0.12?* | $g = 18.65$* |
| 19aavitlq | 2019gip | SNIa-91bg | 0.0315 | $r = 18.52$* | 19abpyqog | 2019oba | SNII | 0.0310 | $r = 18.85$* |
| 18aboabxv | 2018fob | SNIc | 0.0290 | $r = 18.64$* | 18adachwf | 2018lev | SNIIP | 0.0290 | $r = 18.84$* |
| 19aaksrgj | 2019bbd | SNIa | 0.0859 | $g = 18.73$* | 20aavpwxl | 2020hzk | *SNIa?* | 0.0859 | $r = 18.82$* |

*Asterisks indicate brightest magnitude is fainter than 18.5 mag.

## 2.2 Classification for SN 2019uej (ZTF19acnwelq)

SN 2019uej has a light curve with 8 epochs over ~ 50 days, 6 of them during the transient's rise. SN 2019uej appears to have a color of $g-r\sim-0.2$ mag during the rise, and the light curve[8] appears to be consistent with a SN Ia, like its sibling SN 2019sik (ZTF19accobqx). Two pre-max spectra were obtained of SN 2019uej with the P60+SEDM; they are quite noisy but not inconsistent with a SN Ia at $z \sim 0.10$ (i.e., they show potential signatures of Si II, and not hydrogen). Thus, it appears likely that SN 2019uej was a Type Ia SN, the same as its sibling SN 2019sik. The spectra of sibling SN 2019sik have a higher signal-to-noise ratio and indicate a redshift $z \sim 0.1$ (Dahiwale et al. 2019), but using this redshift results in a peak absolute brightness that is overluminous by 0.5–0.8 magnitudes (for both SNe, since they have very similar peak apparent brightnesses).

## 2.3 Classification for SN 2020hzk (ZTF20aavpwxl)

SN 2020hzk has a fairly well-sampled ZTF light curve (11 epochs in 40 days)[9]. It exhibits a rise time of ~ 15 days; a color of $g-r \sim 0$ mag until peak, after which it increases to $g - r \sim 1$ mag by two weeks

---

[8] A publicly viewable light curve for SN 2019uej can be found at `https://lasair.roe.ac.uk/object/ZTF19acnwelq/`.

[9] The light curve of SN 2020hzk is publicly viewable at `https://alerce.online/object/ZTF20aavpwxl`

after peak; a decline rate of $\Delta g \sim 1.2$ mag during the 15 days after peak brightness; and an absolute peak brightness of $g \sim -19.05$ mag. No spectra were obtained of this object, but its light curve suggests it is a Type Ia SN, the same as its sibling SN 2019bbd (ZTF19aaksrgj).

### 2.4 Additional ZTF Sibling SNe

There are several other SN sibling pairs in the ZTF public survey which were not in the BTS sample, or occurred outside our time boundary, which we mention here. The SN Ia sibling pairs ZTF20abatows/ZTF20abcawtk, ZTF20aaeszsm/ZTF20abujoya, and ZTF19aakluwr/ZTF20acpqbue are not in our sample because in all cases, the latter SN of the two did not pass either the BTS filter or the quality and purity cuts applied by Perley et al. (2020a). Biswas et al. (2021) present two ZTF SN Ia siblings, SNe 2019lcj and 2020aewj, in the same host galaxy at $z = 0.0541$, within $0.6''$ of each other (and so both have the ZTF identifier ZTF19aambfxc). SN 2019lcj did not pass the BTS filter and so was not considered for this work. Biswas et al. (2021) find that one of the siblings experienced significantly more dust extinction and reddening, a fact that they use to draw conclusions about the dust content of the host galaxy and also to demonstrate a robust correction. We also note the work of Soraisam et al. (2021), who followed up on the curious case of ZTF20aamibse/AT 2020caa, which appeared to exhibit a second outburst in 2021 of similar brightness. They show that this second event is a SN Ia, offset by $\sim 1.3''$ from the original AT 2020caa, and furthermore show that the first event is also likely a SN (and not, e.g., a precursor outburst).

## 3 SN SIBLINGS AND PARENT GALAXIES

For the SN siblings in our main sample of ZTF BTS events which reached a peak brightness of at least of $r{\sim}18.5$ mag, we analyze each pair and host galaxy in turn. We also searched for past events in these host galaxies, discovered by surveys other than ZTF, but only found additional siblings for SNe 2019ehk & 2020oi in grand design spiral galaxy M100, as discussed in Section 3.1.

### 3.1 SNe 2019ehk & 2020oi: A IIb–Ic Pair and their Older Siblings in Grand Design Spiral M100

SN 2019ehk (ZTF19aatesgp) was first discovered and reported to the Transient Name Server (TNS[10]) by Mr. Jaroslaw Grzegorzek on 2019 Apr 29 with a clear-filter brightness of $\sim 16.5$ mag (Grzegorzek 2019). Being so bright and in a nearby host galaxy Messier 100, SN 2019ehk was detected by many other professional and amateur surveys, and spectroscopic monitoring began with its prompt classification as a SN Ib (Dimitriadis et al. 2019). However, as can be seen in the top-left panel of Figure 3 the spectrum of SN 2019ehk evolved over time to resemble a SN IIb (H and He absorption) and then strong Ca ɪɪ features emerge. Subsequent multi-wavelength follow-up out to late phases revealed SN 2019ehk to be unlike typical “Ca-rich" transients associated with old stellar populations (Kasliwal et al. 2012), and to likely be the core-collapse of a low-mass star exploding into a dense circumstellar material composed of its ultra-stripped envelope (e.g., Nakaoka et al. 2020; Jacobson-Galán et al. 2020; De et al. 2020a).

SN 2020oi (ZTF20aaelulu) was discovered by ZTF and first reported to the TNS by the ALeRCE[11] broker on 2020 Jan 07 (Forster et al. 2020b), and classified as a Type Ic with an optical spectrum obtained within 2 days with the Goodman spectrograph at SOAR Observatory (Siebert et al. 2020). The discovery of SN 2020oi was more than ten days before peak $g$ band brightness, and rapid follow-up with Swift UVOT revealed a rising UV source (Ho et al. 2020). SN 2020oi was also subsequently detected by optical imaging surveys ATLAS (Tonry et al. 2018a), the Young Supernova Experiment (YSE, using PanSTARRS1; Jones et al. 2020), and Gaia Alerts (Wyrzykowski et al. 2012), and monitored with optical spectroscopy (e.g., Dutta et al. 2020). Optical photometric and spectroscopic follow-up was also obtained and reported by Pignata et al. (2020) and Dutta et al. (2020).

Follow-up in the radio in the days after discovery revealed a potential 10 GHz source and a confirmed 44 GHz source with the VLA (Horesh & Sfaradi 2020a,b), a detection at 15.5 GHz with AMI-LA (Sfaradi et al. 2020), and a detection at 5.1 GHz with e-MERLIN (Moldon et al. 2020). Horesh et al. (2020) presents the ZTF optical observations as well as radio data for SN 2020oi; they model the radio observations and find that the density structure of the circumstellar material in the progenitor system might not follow the expected $r^{-2}$ distribution, but that otherwise SN 2020oi is a standard Type Ic SN. Optical and near-infrared observations of SN Ic 2020oi are also presented and analyzed by Rho et al. (2020), who confirm it to be a normal representative of the Type Ic class but which, uniquely, exhibits signatures of dust formation starting >60 days after explosion.

The host galaxy, Messier 100, has produced five other supernovae in the last 120 years: 1901B (SN I), 1914A (untyped), 1959E (SN I), 1979C (SN II), and 2006X (SN Ia; Ponticello et al. 2006; Quimby et al. 2006). The classifications for SNe 1901B, 1959E, and 1989C are compiled in Barbon et al. (1999). The positions of all five previous SNe are shown along with SNe 2019ehk and 2020oi in the top-left panel of Figure 1. The presence of three confirmed core-collapse SNe (Ic, IIb, and II) indicates a host galaxy with active star formation, which is obviously the case for face-on spiral galaxy M100.

Aramyan et al. (2016) used a sample of 215 (non-sibling) SNe to show that, in grand design spirals like M100, SNe from higher-mass progenitors occur closer to the leading edges of spiral arms due to the shock-triggered star formation that occurs there (inside the corotation radius, the leading edges are the inner edges of spiral arms). The corotation radius for M100 is ∼10.5 kpc (e.g., Scarano & Lépine 2013), which is equivalent to the image boundaries in the top-left panel of Figure 1. Despite M100 being a prolific producer of SNe it is difficult to see (let alone confirm) this trend with its seven siblings, although SN II 1979C does appear on the outer edge of its spiral arm. Despite SN Ia 2006X appearing near the inner edge of that same arm, it does not appear to be related to star formation activity (the bright clumps).

However, the top-left panel of Figure 1 does clearly show that the SNe from higher-mass progenitor stars, SN 2019ehk (IIb) and SN 2020oi (Ic) occurred closer to the core of M100. This agrees with previous large-sample analysis of (non-sibling) SNe-host offsets, which suggested that the regions of high stellar density are more efficient at forming the high stellar mass binaries that produce SNe Ic (e.g., Kelly & Kirshner 2012; Kelly et al. 2014). However, recent results from the Palomar Transient Factory show that the distribution of host offsets are very similar for all types of CC SNe (e.g., Schulze et al. 2020, their Fig. 12). For these siblings, SN Ic 2020oi in par-

---

[10] `https://www.wis-tns.org/`

[11] Förster et al. (2020a); `http://alerce.science/`

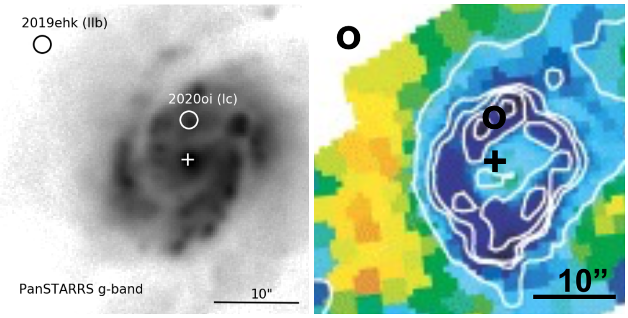

**Figure 4.** *Left:* The central region of M100 in PanSTARRS $g$ band, with logarithmic scaling. *Right:* From Figure 7 of Allard et al. (2006), the [O iii]/H$\beta$ emission line ratio (dark blue corresponds to a ratio of $\sim 10^{-3}$, light blue to $\sim 10^{-1}$) with H$\beta$ contours over-plotted in white. We have added the locations of SNe 2020oi and 2019ehk. Lower ratios of the [O iii]/H$\beta$ emission line ratio indicate active star formation, and SN 2020oi clearly originated in M100's circumnuclear ring of cool gas.

ticular is clearly associated with the cool gas ring of star formation around the nucleus of M100, as shown in Figure 4: the left panel is a zoom-in on the central region of the PanSTARRS image from the top-left panel of Figure 1, whereas the right panel is from Figure 7 of Allard et al. (2006), a map of the [O iii]/H$\beta$ ratio with H$\beta$ contours to which we have added the locations of SN 2020oi and 2019ehk. To summarize, both siblings SN IIb 2019ehk and SN Ic 2020oi appear to be normal representatives of their class and associated with active star formation in M100, as expected.

### 3.2 SNe 2018big & 2019nvm: Distance Estimates with a Ia–IIP Sibling Pair

SN 2018big (ZTF18aasdted) was discovered on 2018 May 10 at 18.96 mag in the orange filter by the ATLAS survey (Tonry et al. 2018b), and subsequently detected by the ZTF and PanSTARRS (Chambers et al. 2016) surveys. An optical spectrum with the P60+SEDM obtained on 2018 May 15 (shown in Figure 3), was used to classify SN 2018big as a Type Ia supernova (Fremling et al. 2018a).

We apply the SALT2 light curve fitter (Guy et al. 2007) to the ZTF $g$- and $r$-band photometry. SALT2 returns light curve fit parameters of $x_1 = 0.72$, which translates to a light curve decline rate parameter of $\Delta m_{15}(B) = 0.98$ mag, which is at the low end of the SN Ia decline-rate distribution and indicates that SN 2018big was also likely more luminous than average. SALT2 returns light curve fit parameters of the apparent $B$-band magnitude, $m_B = 15.8$ mag, and the color excess, $c = 0.11$. These values agree also with those reported for SN 2018big (ZTF18aasdted) in Yao et al. (2019, their Table 3).

The SALT2 parameters are related to the distance modulus, $\mu$, via $\mu = m_B + \alpha * x_1 - \beta * c - M_B$, where $\alpha$ and $\beta$ are the width-luminosity and colour-luminosity relation coefficients and $M_B$ is the absolute $B$-band magnitude from an independent calibration of SNe Ia. Using the $\alpha$ and $\beta$ relation coefficient from the ZTF Year 1 sample (Dhawan et al. 2021), we get a corrected peak apparent magnitude of 15.498 ± 0.04 mag. We take the $M_B$ value of -19.326 ±0.03 mag from the tip of the red giant branch (TRGB) calibration of the SN Ia luminosity (Freedman et al. 2019) to get a distance modulus of 34.824 ± 0.055 (statistical) mag. Adding a systematic error of 0.15 mag for the intrinsic scatter of SN Ia we get $\mu = 34.824 \pm 0.16$ mag. We note that using a calibration of $M_B$ from Cepheid variables (Riess et al. 2019) gives a $\mu$ value that is 0.1 mag lower. In the following description of the distance for SN II-P 2019nvm, we assume an $H_0$ of 70 kms$^{-1}$Mpc$^{-1}$, which is what the TRGB calibration yields. Hence, for the direct comparison of the SN II-P and SN Ia distance (see below), we use the value of $\mu$ derived using $M_B$ from the TRGB value.

SN 2019nvm (ZTF19abqhobb) first was discovered on 2019 Aug 19 in ZTF imaging with an $r$ band brightness of 18.3 mag and reported by the AMPEL[12] broker (Nordin et al. 2019c), and subsequently detected by ATLAS and PanSTARRS. As described by Hiramatsu et al. (2019), optical spectroscopy obtained with the FLOYDS instrument by the Las Cumbres Observatory Global SN Project on 2019 Aug 20 revealed a blue continuum and potential flash ionization features, classifying SN 2019nvm as a Type II. The spectrum obtained by ZTF on 2019 Nov 2 with the SEDM+P60 confirms this classification with its clear P-Cygni profile for H$\alpha$ (Figure 3). The ZTF light curve shown in Figure 2 exhibits the typical slow decline of Type IIP SNe.

Nance et al. (2021) apply the SN IIP distance estimate method of Nugent et al. (2006) to their time series of $g$, $r$, and $i$-band photometry and five optical spectra between 10 and 90 days after explosion. They find an intrinsic $I$-band magnitude of $-17.84 \pm 0.14$ mag at 50 days, a distance modulus of $\mu = 34.95 \pm 0.26$ mag and a distance of $D = 97.6 \pm 12$ Mpc for SN 2019nvm. SN 2019nvm will be included in a full cosmological analysis of ZTF SNe IIP in a forthcoming publication. Now we can make a direct comparison of the two SN-derived distances for the parent galaxy: $\mu_{Ia} = 34.824 \pm 0.16$ mag and $\mu_{IIP} = 34.95 \pm 0.26$ mag. These two values are discrepant by only 0.126 mag, and their combined errors are 0.30 mag, so these results have very good agreement within 0.4$\sigma$.

As shown in Figure 1, the parent galaxy (UGC 10858) is oriented at high inclination and both SN Ia 2018big and SN IIP 2019nvm appear to be embedded in the disk with a moderate offset from the host center. The SDSS spectrum for UGC 10858 reveals the signatures of star formation and is the source of the redshift of $z = 0.01815$ (Ahumada et al. 2020). Type Ia and IIP SNe come from older and younger progenitor stars, respectively, and since both stellar populations are present in the disks of spiral galaxies it is not surprising to find them in the same host. Studies of the rates and properties of Type Ia SNe and their host galaxies have established that events associated with younger stellar populations tend to exhibit brighter, bluer, and broader optical light curves (e.g., Hamuy et al. 1995; Sullivan et al. 2006). Indeed, as discussed above, SN 2018big exhibited a slow decline rate (a broader light curve), a traits consistent with SN 2018big being associated with a younger stellar population.

### 3.3 SNe 2018dbg & 2019hyk: Ib/c–IIP Siblings

SN 2018dbg (ZTF18abdffeo) was discovered and first reported by ZTF on 2018 Jun 28 at 18.43 mag in the $r$ band (Fremling 2018), and subsequently detected and reported by Gaia Alerts on 2018 Jul 11. An optical spectrum with the 5.1m Hale Telescope at Palomar Observatory on 2018 Aug 04 (green line, Figure 3) was used to classify SN 2018dbg as a Type Ib/c (Fremling et al. 2018b). De et al. (2020b) describe how, once the host galaxy emission is subtracted from the 2018 Aug 04 spectrum, they could more clearly see photospheric-phase oxygen, calcium, and helium lines in order to classify SN 2018dbg as a Ib-like event. SN 2018dbg does show a broad Ca ii triplet emission feature, but De et al. (2020b) explain that nebular [Ca ii] is not seen and thus SN 2018dbg is rejected from their

---

[12] Nordin et al. (2019a); `https://github.com/AmpelProject/Ampel-contrib-sample`

sample of Ca-rich gap transients. The light curve of SN 2018dbg is poorly sampled but resembles a SN Ib/c in terms of its rise and fall, and has a $g - r$ color at peak brightness of ~0.75 mag, which is consistent with SNe Ib/c as a population (Taddia et al. 2015). As quoted by De et al. (2020b), the peak intrinsic magnitude of SN 2018dbg was $M_r = -16.6$ mag, which is on the faint side but by no means an outlier for the SN Ib/c class (Richardson et al. 2014). All together, SN 2018dbg appears to be a normal Type Ib/c supernova.

SN 2019hyk (ZTF19abajxet) was discovered by the All Sky Automated Survey for SuperNovae (ASAS-SN[13]) on 2019 Jun 22 (Stanek 2019), with a first detection magnitude of 17.1 in the SDSS-$g$ filter. Classification of SN 2019hyk as a Type II was reported by Fraser et al. (2019) using a spectrum from the ACAM instrument on the William Herschel Telescope, as shown in Figure 3 (orange line; the blue line shows a P60+SEDM spectrum from the same night, Fremling et al. 2019a). Fraser et al. (2019) describe how the blue spectrum exhibits a weak, broad emission feature at H$\alpha$ consistent with SNe II, and an emission feature at ~4580 Å (observer-frame) consistent with the high-ionization signatures of shock breakout seen in young core-collapse SNe (e.g., Gal-Yam et al. 2014). The ZTF light curve of SN 2019hyk in Figure 2 exhibits a ~60-day decline of ~0.5 mag in $r$ (and ~1.2 mag in $g$), which is consistent with a plateau and indicates SN 2019hyk is a SN IIP (e.g., Arcavi et al. 2012).

Parent galaxy IC 4397 is a member of the Coma Supercluster (Véron-Cetty & Véron 2010) and has an observed redshift of $z = 0.014737$ (Paturel et al. 2002), and an apparent brightness of ~13.04 mag in the SDSS $r$ band (Abazajian et al. 2005). IC 4397 is classified as an AGN with an active H II nucleus by Véron-Cetty & Véron (2010), and as a Seyfert 2 galaxy based on the infrared properties of its nucleus (Edelson et al. 1987; Pérez García & Rodríguez Espinosa 2001; Ramos Almeida et al. 2007). The SDSS spectrum reveals narrow H$\alpha$, [N II] and [S II], the classic signatures of star formation (SDSS DR14, Abolfathi et al. 2018). In Figure 5 we show an SDSS color image of IC 4397 with the locations of SN Ib/c 2018dbg and SN IIP 2019hyk marked with white circles. As also seen in the PanSTARRS $g$-band image in Figure 1, SN Ib/c 2018dbg is much closer to the core of the host than SN IIP 2019hyk, which is in the outskirts. As discussed in Section 3.1, the central regions with younger stellar populations and/or high stellar densities might be more efficient at forming the high mass binary stars which are the progenitors of SNe Ib/c. Although IC 4397 is an actively star-forming galaxy that has indubitably parented many SNe, we find no public record of any other siblings in IC 4397.

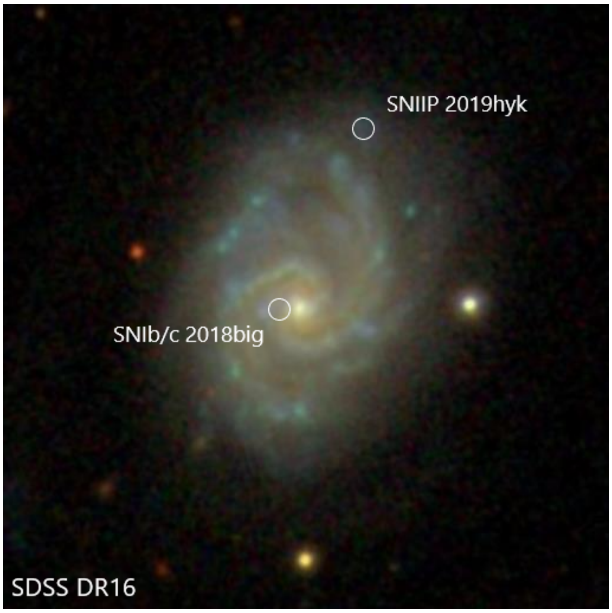

**Figure 5.** An SDSS color image of the host galaxy IC4397 (north-up, east-left, field of view ~2′), with the locations of SN Ib/c 2018dbg and SN IIP 2019hyk marked as open white circles.

### 3.4 SNe 2019bvs & 2019dod: A IIL-IIP Sibling Pair

SN 2019bvs (ZTF19aamhgwm) was first discovered and reported by the ATLAS survey on 2019 Mar 16 at 18.47 mag in the orange-ATLAS filter (Tonry et al. 2019), and subsequently detected and reported by ZTF and the AMPEL broker, Gaia Alerts, and PanSTARRS. An optical spectrum obtained with the P60+SEDM on 2019 Mar 18, shown in Figure 3, showed the broad H$\alpha$ feature which classified SN 201bvs as a Type II supernova (Fremling et al. 2019b). The light curve of SN 2019bvs in Figure 2 reveals a relatively slower rise to peak and then a steady decline instead of a plateau, indicating that it is a Type IIL and not a IIP.

SN 2019dod (ZTF19aaqdkrm) was first discovered and reported by ZTF on 2019 Apr 13 at 18.59 mag in the $r$ band filter (Fremling 2019), and subsequently detected and reported by ATLAS, MASTER (Lipunov et al. 2016), Gaia Alerts, and PanSTARRS. An optical spectrum from the SPRAT (SPectrograph for the Rapid Acquisition of Transients) at the Liverpool Telescope on 2019 Apr 16 revealed a blue continuum, similar to a young Type II SN (Prentice et al. 2019). Subsequent spectra obtained with the P60+SEDM over the next several days, as shown in Figure 3, reveal emergent broad hydrogen features that further suggest SN 2019dod as a Type II. A plateau phase is clearly seen in the light curve of SN 2019dod in Figure 2, solidifying its classification as a Type IIP SN.

It has been hypothesized that the difference between Type IIP, IIL, and IIb supernovae – which exhibit light curves with a ~100 day plateau, a slow decline (~1 mag in ~60 days), and a fast decline (~1 mag in ~20 days), respectively (Arcavi et al. 2012) – could be the mass of the hydrogen envelope at the time of explosion, with less massive envelopes causing a more rapid decline. This correlation would also indicate a trend with progenitor initial mass and age at the time of core-collapse, as more massive progenitors lose more of their hydrogen envelope and evolve towards collapse more rapidly. Envelope mass as the underlying physical characteristic is supported by analyses of large samples of core collapse SN light curves which show that the Type IIP, IIL, and IIb are not distinct groups, but rather a continuum, as expected for a smooth distribution of envelope masses (Anderson et al. 2014; Faran et al. 2014). Such a trend would result in Type IIP, IIL, and IIb SNe being found in regions with progressively younger stellar populations and more active star formation. This trend was established by Anderson et al. (2012), who use H$\alpha$ emission as a tracer of active star formation in SN host galaxies. In particular, they show that the sites of Type IIL exhibit brighter H$\alpha$ emission than Type IIP SNe.

The host galaxy of SNe 2019bvs and 2019dod is a face-on barred spiral, as seen in the SDSS DR16 (Ahumada et al. 2020) color image shown in Figure 6, which also exhibits clear evidence of star formation in its SDSS spectrum (not shown). As is evident in both Figure 1 and 6, Type IIL SN 2019bvs is located in a bright blue knot

[13] Kochanek et al. (2017); `http://www.astronomy.ohio-state.edu/asassn`

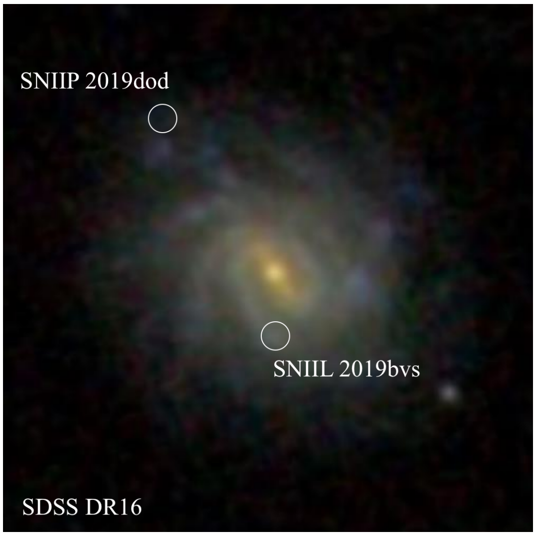

**Figure 6.** An SDSS color image (north-up, east-left, field of view ∼1′) of the face-on barred spiral galaxy hosting SNe 2019dod and 2019bvs.

in a spiral arm, whereas Type IIP SN 2019bvs is in the host galaxy outskirts. In summary, these two siblings exhibit the same trend in which Type IIL SNe are associated with younger stellar populations than Type IIP SNe. As a final note, we remark that other Type IIL SN siblings in multi-SN parent galaxies do not show as clear a trend with active star formation, such as SN 1926A in NGC 4303, SN 1980K in NGC 6946, and SN 1993G in Arp 299, all of which are in regions of fainter surface brightness and/or further from the galaxy's center than some of their SN IIP siblings (Anderson & Soto 2013).

### 3.5 SNe 2019abo & 2020bzv: Type I and Ia Siblings

AT 2019abo (ZTF19aaeiowr) was discovered and first reported by ZTF on 2019 Jan 25 at $r\sim19.08$ mag (Nordin et al. 2019b), and subsequently detected and reported by ATLAS. No spectroscopic classification has been publicly reported for AT 2019abo. A P200+DBSP spectrum obtained 2019 Jan 26, as shown in Figure 3, is dominated by emission from the host galaxy. The light curve for AT 2019abo shown in Figure 2 is sparsely sampled, but with a rise (>15 days) and fall (∼1.25 mag in the first 15 days after peak) consistent with a Type I supernova (i.e., does not exhibit a slow decline or a plateau like Type II SN). If it is a SN Ia, the peak brightness of $g\sim18.25$ mag suggests an extinction of about 1 mag, given a distance modulus of $\mu\sim36.4$ mag based on the host galaxy redshift of $z = 0.043$ from the H$\alpha$ emission line. If it a SN Ib/c, the brightest of which are ∼1 mag fainter than SNe Ia (Li et al. 2011), the host-galaxy extinction could be minimal. Either would be consistent with the SN's location in the disk of its inclined host galaxy (Figure 1). We note that the line-of-sight Milky Way extinction for the sky coordinates of this SN sibling pair is very low, $A_V \approx 0.02$ mag (Schlafly & Finkbeiner 2011).

In Figure 7 we attempt to subtract host galaxy emission from the SN spectrum using an SDSS spectrum of the galaxy. This is inappropriate because the SDSS spectrum includes emission from the host galaxy's core whereas the SN spectrum only includes emission at the SN location (and this host has a bright, compact nucleus). The difference reveals a blue continuum which does not much resemble a SN Ia, and would be more similar to the massive CC events of SN Ib/c – but no distinguishing features are revealed to confirm the type. We thus refer to the type of SN 2019abo as "*SN I?*" in Table 2 to denote the uncertainty in its classification.

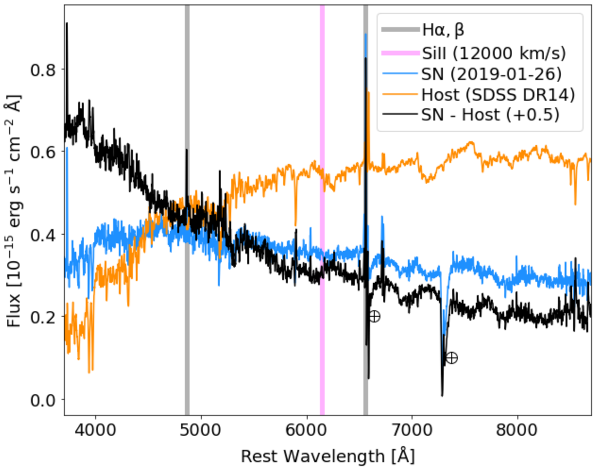

**Figure 7.** The spectrum of AT 2019abo from Fig. 3 (blue), the host galaxy spectrum from SDSS DR14 (Abolfathi et al. 2018; orange), and the host-subtracted SN spectrum (black). Grey and magenta lines mark the locations of hydrogen emission (host galaxy) and potential Si II $\lambda$6355Å absorption (a signature SN Ia feature), respectively. Earth symbols mark two strong atmospheric absorption features.

SN 2020bzv (ZTF20aambbfn) was first detected in ZTF images and reported by the ALeRCE broker on 2020 Feb 7 at 19.6 mag in the $g$ filter (Bauer et al. 2020), and subsequently detected and reported by AMPEL and ATLAS. An optical spectrum obtained on 2020 Feb 12 with the SPRAT at the Liverpool Telescope was used to classify SN 2020bzv as a Type Ia supernova (Perley et al. 2020b). The location of SN 2020bzv was very close to (or projected on) the core of the host galaxy, and the light curve's peak brightness of $g\sim19.25$ mag suggests ∼2 mag of extinction; the light curve is also very clearly reddened. A light curve fit for SN 2020bzv using the SALT2 parameterization (Guy et al. 2007) in the `SNCosmo` package (Barbary et al. 2016) returns parameters $x_1 = -2.35 \pm 0.74$ ($\Delta m_{15} \approx 1.6$ mag) and $c = 0.794 \pm 0.042$ (indicating significant reddening). The spectrum of SN 2020bzv in Figure 3 is also significantly reddened, but the Si II $\lambda$6355 absorption feature clearly identifies the event as Type Ia.

Unfortunately, given the extreme reddening and extinction of SN 2020bzv and the lack of confirmation data for SN 2020abo, these sibling SNe cannot be used for any further science such as constraining the discrepancy in distance estimates (e.g., Gall et al. 2018; Scolnic et al. 2020), investigating correlations between SN Ia and host galaxy properites (e.g., Gallagher et al. 2008), or comparing the dust properties ($R_V$ values) of different sightlines within a given galaxy as done for a pair of ZTF SNe Ia siblings by Biswas et al. (2021), and as done for quasars by, e.g., Falco et al. (1999).

## 4 SN SIBLINGS RELATIVE RATES

In this work we have identified 5 (10) pairs of SN siblings in the ZTF BTS sample of SNe with peak brightness <18.5 (<19.0) mag, which Perley et al. (2020a) have shown to have a spectroscopic completeness of 93% (75%). As described in Section 2, our sample extends about a month before and after the sample used in Perley et al. (2020a), but within that time-frame the completeness statistics still apply.

**Table 3.** The number of BTS SNe by type, for siblings and the full sample. SN 2019abo is counted as a SN Ia here.

| Peak Brightness:<br>Completeness: | <18.5 mag<br>93% | <19 mag<br>75% |
|---|---|---|
| *Siblings Sample* | | |
| Ia | 3 | 8 |
| CC | 7 | 11 |
| II | 5 | 8 |
| Ib/c | 2 | 3 |
| *Full Sample* | | |
| Ia | 939 | 1454 |
| CC | 312 | 495 |
| II | 233 | 371 |
| Ib/c | 79 | 124 |

**Table 4.** Ratios of the number of BTS SNe by type, for siblings and the full sample, with statistical uncertainties derived from the binomial confidence limits of Gehrels (1986). SN 2019abo is counted as a SN Ia, which makes both the CC:Ia and Ib/c:II ratios *lower limits*.

| Peak Brightness: | <18.5 mag | <19 mag |
|---|---|---|
| *Siblings Sample* | | |
| CC:Ia | $2.3^{+3.7}_{-1.4}$ | $1.4^{+0.9}_{-0.7}$ |
| Ib/c:II | $0.4^{+0.8}_{-0.3}$ | $0.4^{+0.5}_{-0.2}$ |
| *Full Sample* | | |
| CC:Ia | 0.33 ± 0.02 | 0.34 ± 0.02 |
| Ib/c:II | 0.34 ± 0.05 | 0.33 ± 0.04 |

The number of SNe that we identify as siblings in the BTS sample and their breakdown by type is listed in Table 3. This measured completeness allows us to do a SN sibling rates analysis. The ratios of BTS SNe by type, CC SN to SN Ia and SN Ib/c to SN II, are provided with 1$\sigma$ statistical errors from Gehrels (1986) in Table 4. For these relative rate ratios, we count SN 2019abo as a Type Ia (although it might be a Type Ib/c) so that the ratio of CC:Ia and Ib/c:II are both *lower limits*.

For our analysis of the relative rates of SN siblings we start with a comparison to Anderson & Soto (2013), who analyzed a sample of 2384 classified, hosted SNe from the Asiago catalog (Barbon et al. 1999) that were detected prior to 2012 May 23. They found that 486 SNe in their sample shared a parent galaxy with one or more siblings: in other words, ∼20% of their SNe had one or more siblings, and ∼10% of their hosts had more than one SN. Many of the SNe in the Asiago catalog come from galaxy-targeted surveys that prioritize the monitoring of galaxies that are most likely to host supernovae, whereas the ZTF is an all-sky non-targeted survey. With ZTF we find only 10 (20) SNe with peak magnitudes <18.5 (<19) mag share parent galaxy, out of 1190 (1857) classified SNe total, or ∼0.8% (∼1%). This difference in the siblings percentage is primarily due to the fact that the ZTF survey includes many more low-mass hosts which have proportionally lower supernova rates and are single parents. In this comparison we must also consider that the Asiago catalog incorporates many detections from as early as 1885, and from a variety of surveys, and that it does not have an internally consistent detection and classification efficiency like the ZTF.

Anderson & Soto (2013) found that core-collapse (CC) SN siblings were likely to be the same type: SN Ib/c with other SN Ib/c, and SN II with other SN II. They explained that this match in sibling type indicates that stars form during bursts of < 10 Myr, i.e., the delay time of a SN II, because continuous (non-bursty) star formation would result in the younger, more massive progenitor stars of Type Ib/c existing in the same regions as the less massive Type II progenitors. Our sample of CC SN siblings does not clearly show this effect, as all three of our Type Ib/c have a Type II sibling, but this could simply be due to our relatively smaller sample size. Anderson & Soto (2013) also demonstrate that their ratio of SN Ib/c to SN II SNe in multiple-SN hosts is 0.338 ± 0.047, higher than their Ib/c:II ratio in single-SN hosts, 0.274 ± 0.021. This statistically significant increase in the Ib/c:II ratio in galaxies that host multiple SNe further illustrates how recent star formation and a young stellar population make a galaxy more likely to become a multiple-SN parent. We list the Ib/c:II ratio for our BTS siblings, $0.40^{+0.8}_{-0.3}$, in Table 4, but find only a small, insignificant increase over the ratio for the full sample 0.34 ± 0.05.

Since SNe Ia are from older stellar populations they occur in both star-forming and elliptical galaxies (e.g., Scannapieco & Bildsten 2005), however core-collapse SNe are almost never found in elliptical galaxies (e.g., Graham et al. 2012; Sanders et al. 2013; Irani et al. 2019; Irani et al. 2021). Although SNe Ia will outnumber CC SNe in a magnitude limited sample like ours, as previously discussed, CC SNe are more likely to appear in the same parent galaxy due to the bursty nature of star formation and their short delay times. Thus, any multiple-SN parent galaxy sample will contain mostly star-forming galaxies, and the CC:Ia ratio will be much higher among siblings. As shown in Table 4, our CC:Ia ratio for the full BTS sample is 0.33 ± 0.02 and for the siblings sample is $2.3^{+3.7}_{-1.4}$, with the <18.5 mag limit. If we expand the sample to include SNe that peaked brighter than <19 mag, we find the CC:Ia ratio among siblings drops to $1.4^{+0.9}_{-0.7}$. The difference between the CC:Ia ratios for the peak <18.5 and <19 mag sibling samples seems large, but the two values are within their combined uncertainties. Anderson & Soto (2013) find a ratio of CC:Ia events of 1.149 ± 0.052 in single-SN hosts, and a larger ratio of 1.946 ± 0.186 in multiple-SN host galaxies. Although both surveys see the increase in the CC:Ia ratio in multiple-SN parent galaxies, the markedly lower CC:Ia ratio in the ZTF BTS full sample, 0.33, compared to the CC:Ia ratio in the single-SN host sample of Anderson & Soto (2013), 1.149, is due to both the depth and wide-field nature of the ZTF survey.

Since we have a magnitude-limited sample with high completeness, we can use the difference in the co-moving volumes for ZTF BTS SNe CC and SNe Ia to estimate the *intrinsic* ratios. Assuming average peak intrinsic brightness for Type Ia and II SNe are −19 and −17 mag respectively, and a flat cosmology with $H_0 = 70$ km s$^{-1}$ Mpc$^{-1}$ and $\Omega_M = 0.3$, the co-moving volume within which they reach a peak apparent brightness of <18.5 mag are 0.110 and 0.009 Gpc$^3$, respectively. Thus, to convert the observed CC:Ia ratios in Table 4 into intrinsic ratios, we multiple by a factor of 0.110/0.009 = 12.2. Based on this we estimate an intrinsic CC:Ia ratio for siblings and the full sample to be approximately ∼28 and ∼4, respectively.

## 5 CONCLUSIONS

These five ZTF sibling pairs contribute to a growing amount of literature demonstrating the use of SNe – and SN siblings in particular – as cosmic lighthouses: signals of the characteristics of unresolved stellar populations and interstellar material in distant galaxies. With our sample from ∼2 years of the ZTF public survey we have focused on the unique aspects of each family, and provided individual analyses of the siblings and their parent galaxies. In general we find that the

SNe from more massive progenitor stars explode nearer the cores of their host galaxies, and/or in regions with more active star formation, as expected. We have also provided the first comparative rates analysis of SN sibling rates in a complete population from an unbiased, well-characterized survey. We find a lower ratio of CC SN to SN Ia than past surveys which targeted specific galaxies in order to maximize the number of SN detections – and as the most common type of SN is CC, it is not surprising that past surveys found more CC SNe.

With our small sample there is not much significance in confirming the expected locations of SNe II *vs.* SNe Ib/c in a few hosts, and it would not have been surprising to find a few events that did not meet expectations. We highlight these trends in order to exemplify the kind of information that SN siblings bring to the broader discussion of progenitor populations, but emphasize that the ZTF SNe cannot confirm (or exclude) any particular models – yet.

As ZTF continues over the next few years, the rate of discovery of ZTF SN siblings will continue to increase, and we will be able to shift our focus from individual families to analyses of the larger sample. Based on the first two years of ZTF BTS SN siblings, for each new year of ZTF survey, 5 new siblings are identified *per past year of survey* in the sample with peak brightness <18.5 mag. Thus at the end of year 2 we have 10 siblings; at the end of year 3 we expect another 10 new siblings for a total of 20; at the end of year 4 we expect 15 new siblings for a total of 35; and at the end of year 5 (fall 2023) we expect a total of 55 siblings. In the larger, less complete sample with peak brightness <19 mag we can expect >100 ZTF BTS siblings by the end of 2023. Looking forward to the Rubin Observatory and its 10-year long Legacy Survey of Space and Time (LSST; Ivezić et al. 2019), the detection of millions of SNe will bring the opportunity for significantly larger samples of SN siblings studies at greater cosmological distances and earlier epochs in the cosmic star formation history and the chemical evolution of the universe.

## ACKNOWLEDGEMENTS

Based on observations obtained with the Samuel Oschin Telescope 48-inch and the 60-inch Telescope at the Palomar Observatory as part of the Zwicky Transient Facility project. ZTF is supported by the National Science Foundation under Grant No. AST-1440341 and a collaboration including Caltech, IPAC, the Weizmann Institute for Science, the Oskar Klein Center at Stockholm University, the University of Maryland, the University of Washington, Deutsches Elektronen-Synchrotron and Humboldt University, Los Alamos National Laboratories, the TANGO Consortium of Taiwan, the University of Wisconsin at Milwaukee, and Lawrence Berkeley National Laboratories. Operations are conducted by COO, IPAC, and UW.

SED Machine is based upon work supported by the National Science Foundation under Grant No. 1106171.

The PanSTARRS1 Surveys (PS1) and the PS1 public science archive have been made possible through contributions by the Institute for Astronomy, the University of Hawaii, the PanSTARRS Project Office, the Max-Planck Society and its participating institutes, the Max Planck Institute for Astronomy, Heidelberg and the Max Planck Institute for Extraterrestrial Physics, Garching, The Johns Hopkins University, Durham University, the University of Edinburgh, the Queen's University Belfast, the Harvard-Smithsonian Center for Astrophysics, the Las Cumbres Observatory Global Telescope Network Incorporated, the National Central University of Taiwan, the Space Telescope Science Institute, the National Aeronautics and Space Administration under Grant No. NNX08AR22G issued through the Planetary Science Division of the NASA Science Mission Directorate, the National Science Foundation Grant No. AST-1238877, the University of Maryland, Eotvos Lorand University (ELTE), the Los Alamos National Laboratory, and the Gordon and Betty Moore Foundation.

MLG acknowledges support from the DIRAC Institute in the Department of Astronomy at the University of Washington. The DIRAC Institute is supported through generous gifts from the Charles and Lisa Simonyi Fund for Arts and Sciences, and the Washington Research Foundation.

## DATA AVAILABILITY

The ZTF BTS photometry and classification spectra for all objects used in this work are publicly available via the TNS or alert brokers such as ANTARES, ALeRCE, and Lasair. More information about the ZTF-I data release for the public survey are available via the ZTF website, `https://www.ztf.caltech.edu/`.

## REFERENCES

Abazajian K., et al., 2005, AJ, 129, 1755

Abolfathi B., et al., 2018, ApJS, 235, 42

Ahumada R., et al., 2020, ApJS, 249, 3

Allard E. L., Knapen J. H., Peletier R. F., Sarzi M., 2006, MNRAS, 371, 1087

Anderson J. P., Soto M., 2013, A&A, 550, A69

Anderson J. P., Habergham S. M., James P. A., Hamuy M., 2012, MNRAS, 424, 1372

Anderson J. P., et al., 2014, ApJ, 786, 67

Aramyan L. S., et al., 2016, MNRAS, 459, 3130

Arcavi I., et al., 2012, ApJ, 756, L30

Barbary K., et al., 2016, ] 10.5281/zenodo.168220

Barbon R., Buondí V., Cappellaro E., Turatto M., 1999, A&AS, 139, 531

Bauer F. E., et al., 2020, Transient Name Server Discovery Report, 2020-413, 1

Bellm E. C., et al., 2019, PASP, 131, 018002

Biswas et al. 2021, in prep.

Blagorodnova N., et al., 2018, PASP, 130, 035003

Burns C. R., et al., 2020, ApJ, 895, 118

Chambers K. C., et al., 2016, arXiv e-prints, p. arXiv:1612.05560

Dahiwale A., Fremling C., Dugas A., 2019, Transient Name Server Classification Report, 2019-2115, 1

De K., Fremling U. C., Gal-Yam A., Kasliwal M. M., Kulkarni S. R., 2020a, arXiv e-prints, p. arXiv:2009.02347

De K., et al., 2020b, ApJ, 905, 58

Dhawan et al. 2021, in prep.

Dimitriadis G., Siebert M. R., Kilpatrick C. D., Rojas-Bravo C., Foley R. J., Rich M., 2019, Transient Name Server Classification Report, 2019-675, 1

Dutta A., Kumar B., Anupama G. C., Sahu D., Sujith D. S., Singh A., 2020, The Astronomer's Telegram, 13404, 1

Edelson R. A., Malkan M. A., Rieke G. H., 1987, ApJ, 321, 233

Falco E. E., et al., 1999, ApJ, 523, 617

Faran T., et al., 2014, MNRAS, 445, 554

Förster F., et al., 2020a, arXiv e-prints, p. arXiv:2008.03303

Forster F., et al., 2020b, Transient Name Server Discovery Report, 2020-67, 1

Fraser M., Eappachen D., Maguire K., Jonker P., 2019, Transient Name Server Classification Report, 2019-1061, 1

Freedman W. L., et al., 2019, ApJ, 882, 34

Fremling C., 2018, Transient Name Server Discovery Report, 2018-915, 1

Fremling C., 2019, Transient Name Server Discovery Report, 2019-586, 1

Fremling C., Sharma Y., Dugas A., 2018a, Transient Name Server Classification Report, 2018-1071, 1

Fremling C., Dugas A., Sharma Y., 2018b, Transient Name Server Classification Report, 2018-1142, 1

Fremling C., Dugas A., Sharma Y., 2019a, Transient Name Server Classification Report, 2019-2826, 1

Fremling C., Dugas A., Sharma Y., 2019b, Transient Name Server Classification Report, 2019-411, 1

Fremling C., et al., 2020, ApJ, 895, 32

Gal-Yam A., et al., 2014, Nature, 509, 471

Gall C., et al., 2018, A&A, 611, A58

Gallagher J. S., Garnavich P. M., Caldwell N., Kirshner R. P., Jha S. W., Li W., Ganeshalingam M., Filippenko A. V., 2008, ApJ, 685, 752

Gehrels N., 1986, ApJ, 303, 336

Graham M. L., et al., 2012, ApJ, 753, 68

Graham M. J., et al., 2019, PASP, 131, 078001

Grzegorzek J., 2019, Transient Name Server Discovery Report, 2019-666, 1

Guy J., et al., 2007, A&A, 466, 11

Hamuy M., Phillips M. M., Maza J., Suntzeff N. B., Schommer R. A., Aviles R., 1995, AJ, 109, 1

Hiramatsu D., Arcavi I., Burke J., Howell D. A., McCully C., Pellegrino C., Valenti S., 2019, Transient Name Server Classification Report, 2019-1557, 1

Ho A. Y. Q., Schulze S., Perley D., Sollerman J., Yang Y., Yaron O., Kasliwal M. M., 2020, Transient Name Server AstroNote, 8, 1

Horesh A., Sfaradi I., 2020a, Transient Name Server AstroNote, 9, 1

Horesh A., Sfaradi I., 2020b, Transient Name Server AstroNote, 10, 1

Horesh A., et al., 2020, ApJ, 903, 132

Hosseinzadeh G., et al., 2017, ApJ, 845, L11

Irani I., et al., 2019, ApJ, 887, 127

Irani et al. 2021, in prep.

Ivezić Ž., et al., 2019, ApJ, 873, 111

Jacobson-Galán W. V., et al., 2020, ApJ, 898, 166

Jones D. O., et al., 2020, arXiv e-prints, p. arXiv:2010.09724

Kasliwal M. M., et al., 2012, ApJ, 755, 161

Kelly P. L., Kirshner R. P., 2012, ApJ, 759, 107

Kelly P. L., Filippenko A. V., Modjaz M., Kocevski D., 2014, ApJ, 789, 23

Kochanek C. S., et al., 2017, PASP, 129, 104502

Li W., et al., 2011, MNRAS, 412, 1441

Lipunov V., et al., 2016, in Revista Mexicana de Astronomia y Astrofisica Conference Series. pp 42–47

Magnier E. A., et al., 2020, ApJS, 251, 3

Masci F. J., et al., 2019, PASP, 131, 018003

Moldon J., Horesh A., Perez-Torres M., Sfaradi I., Lundqvist P., 2020, The Astronomer's Telegram, 13448, 1

Nakaoka T., et al., 2020, arXiv e-prints, p. arXiv:2005.02992

Nance et al. 2021, in prep.

Nordin J., et al., 2019a, A&A, 631, A147

Nordin J., Brinnel V., Giomi M., Santen J. V., Gal-yam A., Yaron O., Schulze S., 2019b, Transient Name Server Discovery Report, 2019-141, 1

Nordin J., Brinnel V., Giomi M., Santen J. V., Gal-Yam A., Yaron O., Schulze S., 2019c, Transient Name Server Discovery Report, 2019-1546, 1

Nugent P., et al., 2006, ApJ, 645, 841

Paturel G., Dubois P., Petit C., Woelfel F., 2002, LEDA, p. 0

Pérez García A. M., Rodríguez Espinosa J. M., 2001, ApJ, 557, 39

Perley D. A., et al., 2020a, ApJ, 904, 35

Perley D. A., Taggart K., Dahiwale A., Fremling C., 2020b, Transient Name Server Classification Report, 2020-561, 1

Pignata G., et al., 2020, The Astronomer's Telegram, 13396, 1

Ponticello N. J., et al., 2006, IAU Circ., 8667, 1

Prentice S. J., Maguire K., Skillen K., Magee M. R., Clark P., 2019, Transient Name Server Classification Report, 2019-589, 1

Quimby R., Brown P., Gerardy C., Odewahn S. C., Rostopchin S., 2006, Central Bureau Electronic Telegrams, 393, 1

Ramos Almeida C., Pérez García A. M., Acosta-Pulido J. A., Rodríguez Espinosa J. M., 2007, AJ, 134, 2006

Rho J., et al., 2020, arXiv e-prints, p. arXiv:2010.00662

Richardson D., Jenkins Robert L. I., Wright J., Maddox L., 2014, AJ, 147, 118

Riess A. G., Casertano S., Yuan W., Macri L. M., Scolnic D., 2019, ApJ, 876, 85

Rigault M., et al., 2019, A&A, 627, A115

Sanders N. E., et al., 2013, ApJ, 769, 39

Scannapieco E., Bildsten L., 2005, ApJ, 629, L85

Scarano S., Lépine J. R. D., 2013, MNRAS, 428, 625

Schlafly E. F., Finkbeiner D. P., 2011, ApJ, 737, 103

Schulze S., et al., 2020, arXiv e-prints, p. arXiv:2008.05988

Scolnic D., et al., 2020, ApJ, 896, L13

Sfaradi I., Williams D., Horesh A., Fender R., Green D., Titterington D., Perrott A. Y., 2020, Transient Name Server AstroNote, 11, 1

Siebert M. R., Kilpatrick C. D., Foley R. J., Cartier R., 2020, Transient Name Server Classification Report, 2020-90, 1

Soraisam M., Matheson T., Lee C.-H., 2021, arXiv e-prints, p. arXiv:2103.09937

Stanek K. Z., 2019, Transient Name Server Discovery Report, 2019-1053, 1

Sullivan M., et al., 2006, ApJ, 648, 868

Taddia F., et al., 2015, A&A, 574, A60

Thöne C. C., Michałowski M. J., Leloudas G., Cox N. L. J., Fynbo J. P. U., Sollerman J., Hjorth J., Vreeswijk P. M., 2009, ApJ, 698, 1307

Tonry J. L., et al., 2018a, PASP, 130, 064505

Tonry J., et al., 2018b, Transient Name Server Discovery Report, 2018-609, 1

Tonry J., et al., 2019, Transient Name Server Discovery Report, 2019-385, 1

Véron-Cetty M. P., Véron P., 2010, A&A, 518, A10

Wyrzykowski Ł., Hodgkin S., Blogorodnova N., Koposov S., Burgon R., 2012, in 2nd Gaia Follow-up Network for Solar System Objects. p. 21 (`arXiv:1210.5007`)

Yao Y., et al., 2019, ApJ, 886, 152

Zwicky F., 1938, ApJ, 88, 529